nature cell biology

Chromatin relaxation in response to DNA double-strand breaks is modulated by a novel ATM- and KAP-1 dependent pathway

Yael Ziv[1,5], Dana Bielopolski[1], Yaron Galanty[1], Claudia Lukas[2], Yoichi Taya[3], David C. Schultz[4], Jiri Lukas[2], Simon Bekker-Jensen[2], Jiri Bartek[2] and Yosef Shiloh[1,5]

The cellular DNA-damage response is a signaling network that is vigorously activated by cytotoxic DNA lesions, such as double-strand breaks (DSBs)[1]. The DSB response is mobilized by the nuclear protein kinase ATM, which modulates this process by phosphorylating key players in these pathways[2]. A long-standing question in this field is whether DSB formation affects chromatin condensation. Here, we show that DSB formation is followed by ATM-dependent chromatin relaxation. ATM's effector in this pathway is the protein KRAB-associated protein (KAP-1, also known as TIF1β, KRIP-1 or TRIM28), previously known as a corepressor of gene transcription[3,4]. In response to DSB induction, KAP-1 is phosphorylated in an ATM-dependent manner on Ser 824. KAP-1 is phosphorylated exclusively at the damage sites, from which phosphorylated KAP-1 spreads rapidly throughout the chromatin. Ablation of the phosphorylation site of KAP-1 leads to loss of DSB-induced chromatin decondensation and renders the cells hypersensitive to DSB-inducing agents. Knocking down *KAP-1*, or mimicking a constitutive phosphorylation of this protein, leads to constitutive chromatin relaxation. These results suggest that chromatin relaxation is a fundamental pathway in the DNA-damage response and identify its primary mediators.

DSBs in DNA are induced by cellular metabolites, normal DNA transactions and environmental agents, such as ionizing radiations and radiomimetic chemicals. DSBs, which present a serious threat to cellular homeostasis and life, swiftly evoke the DNA damage response — an elaborate signalling network of repair mechanisms, cell-cycle checkpoints, apoptotic pathways and many as yet undefined stress responses[1,5,6]. Genetic defects in this system usually lead to genomic-instability syndromes that almost invariably involve predisposition to cancer.

The chief activator of this massive response is the nuclear protein kinase ATM. ATM is missing or inactivated in patients with the genomic instability syndrome ataxia-telangiectasia (A-T). Following DSB formation, ATM is activated, a portion of the protein is recruited to the damage sites and it then phosphorylates a multitude of substrates, each of which takes part in a damage response pathway[2,6]. ATM belongs to a family of proteins, most of them protein kinases, which contain a phosphatidylinositol 3-kinase-like domain. A close ally of ATM is another member of this family, ATR. ATR responds primarily to UV lesions and stalled replication forks, but is also activated at a later stage of the DSB response and is thought to maintain the phosphorylation of certain ATM substrates[7].

Further understanding of the DNA-damage response requires the elucidation of new branches of this network. Phospho-specific antibodies are a useful tool for identifying novel kinase substrates. These antibodies are designed to monitor the phosphorylation of specific sites on known substrates, but cross-reaction with similar sites on other substrates may allow a single antibody to detect the phosphorylation of several proteins. The target sites of ATM and ATR share a common core, SQ or TQ — the phosphorylated serines or threonines are usually followed by a glutamine. Proteins that share as few as one or two residues flanking this motif can potentially create a common epitope. We noticed such cross-reactivity of an antibody that had been raised against phosphorylated Ser 407 of the oncogenic protein Mdm2.

Ser407 of Mdm2, which is part of an SQ motif, is not phosphorylated by ATM in response to DSBs, but rather by ATR, several hours after treatment with replication blockers[8]. This ATR-mediated phosphorylation is unlike most DSB-induced phosphorylations mediated by ATM, which appear minutes after damage induction. However, it was observed that the corresponding phospho-specific antibody did detect rapid, vigorous phosphorylation of another protein, with a migration pattern that was different from Mdm2, shortly after treatment of human cells with the DSB-inducing chemical neocarzinostatin (NCS; see Supplementary Information, Fig. S1a). Furthermore, this reaction was observed in Mdm2-deficient cells (data not shown). Contrary to Mdm2 phosphorylation on Ser 407 following replication block, this phosphorylation

[1]The David and Inez Myers Laboratory for Genetic Research, Department of Molecular Genetics and Biochemistry, Sackler School of Medicine, Tel Aviv University, Tel Aviv 69978, Israel. [2]Danish Cancer Society, Institute of Cancer Biology and Centre of Genotoxic Stress Research, DK-2100 Copenhagen, Denmark. [3]Radiobiology Division, National Cancer Center Research Institute, Tsukiji 5-1-1, Chuo-ku, Tokyo 104-0045, Japan. [4]Case Western Reserve University, Department of Pharmacology, 10900 Euclid Avenue, Cleveland, OH 44106-4965, USA.
[5]Correspondence should be addressed to Y.Z. or Y.S. (e-mail: yaelz@post.tau.ac.il; yossih@post.tau.ac.il)

Received 22 March 2006; accepted 4 July 2006; published online 23 July 2006; DOI: 10.1038/ncb1446

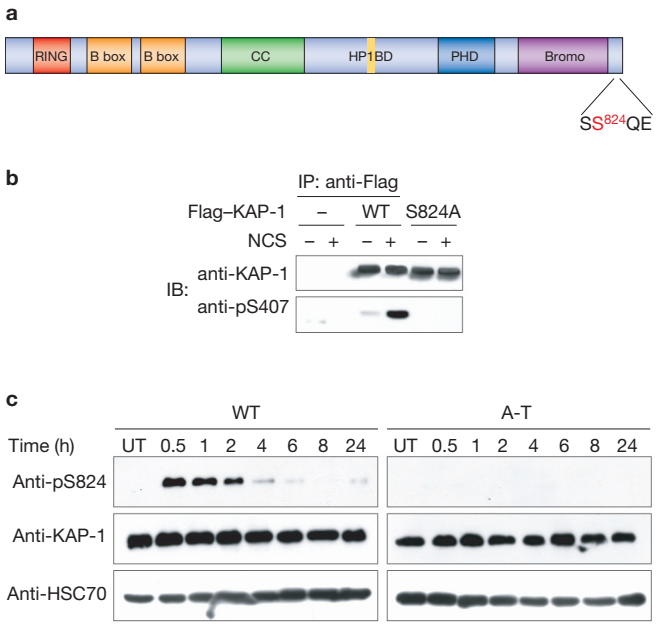

Figure 1 KAP-1 is a novel ATM substrate in the DNA-damage response. (**a**) Schematic representation of the domains of KAP-1. CC, coiled–coil; HP1BD, HP1-binding domain. The PHD and BROMO domains are typical of proteins that interact with chromatin and are involved in chromatin modifications. ATM's target, Ser 824, is at the carboxy-terminus of the protein. (**b**) Detection of KAP-1 phosphorylation in cells using a specific anti-phospho antibody. Wild-type and mutant (S824A) Flag-tagged KAP-1 was ectopically expressed in HEK293 cells. Following treatment with 200 ng ml^{-1} NCS for 30 min, ectopic KAP-1 was immunoprecipitated using an anti-Flag antibody and the immune complexes were blotted with anti-KAP-1 and anti-pS824 antibodies. See Supplementary Information, Fig. S2b for further characterization of the anti-pS824 antibody. (**c**) Rapid kinetics and ATM dependence of KAP-1 phosphorylation following ionizing radiation treatment. Wild-type and lymphoblastoid cells were irradiated with 2 Gy X-rays and cellular extracts were blotted with the indicated antibodies at various times after irradiation.

peaked rapidly and declined within several hours with kinetics typical of many ATM substrates and was ATM-dependent (see Supplementary Information, Fig. S1b, c).

The phosphorylated protein was identified as KAP-1 using biochemical fractionation and mass spectrometric analysis. Importantly, KAP-1 contains the sequence SS824QE, which is identical to that surrounding Ser 407 of MDM2 (SS407QE) and contains the epitope potentially recognized by the antibody on phosphorylation of Ser 824 (Fig. 1a). Reciprocal immunoprecipitation experiments suggested that KAP-1 was indeed the protein detected by the antibody and indicated that it was quantitatively phosphorylated in response to DSBs (see Supplementary Information, Fig. S2a). The reactivity of the phospho-specific antibody with phosphorylated Ser 824 of KAP-1 was confirmed using ectopically expressed wild-type KAP-1, and a mutant protein (KAP-1^{S824A}) in which the phosphorylation site had been abolished (Fig. 1b). ATM-dependent phosphorylation of KAP-1 was characterized by rapid kinetics, peaking 30–60 min after DSB induction and largely disappearing after several hours (Fig. 1c). A longer time course and variable degrees of KAP-1 phosphorylation were observed in response to treatments with UV irradiation, the methylating agent methyl methane sulfonate (MMS) and the replication blocker hydroxyurea (see Supplementary Information, Fig. S3), probably reflecting secondary formation of DSBs. At the range of treatment doses used in this study, KAP-1 phosphorylation did not seem to require the presence of the DNA-damage response proteins MDC-1, BRCA1 and 53BP1 (data not shown).

KAP-1 is a nuclear phosphoprotein with a relative molecular mass of 97,000 (M_r = 97 K) and is known as a universal corepressor of gene transcription[3,4,9]. KAP-1 acts by physically associating with a subclass of the zinc-finger DNA-binding proteins, which contain a KRAB (Kruppel-associated box) domain and repress transcription from RNA polymerase I, II and III promoters. KAP-1 is a member of the TRIM family of proteins[11], characterized by a conserved tripartite motif containing a RING, B1 box, B2 box and coiled–coil motifs (also called an RBCC domain; Fig. 1a). KAP-1 binds to the KRAB domain through this tripartite motif and concomitantly associates with members of the heterochromatin protein 1 (HP1) family, which participate in chromatin packaging and in particular heterochromatin formation. HP1 recruitment to chromatin is enhanced by methylation of histone H3 on K9 by a KAP-1-associated histone methyltransferase SETDB1 (ref. 12). This protein complex induces local heterochromatinization and consequently transcriptional repression[13]. KAP-1 is an essential protein involved in early developmental processes and its ablation in mice results in embryonic lethality[14].

To examine the functional significance of KAP-1 phosphorylation, we stably knocked down cellular *KAP-1* using RNA interference (RNAi) and complemented the cells by stable expression of siRNA-resistant, ectopic *KAP-1* in wild-type and mutant versions containing S824A and S824D substitutions. The S824D mutant is expected to mimic the phosphorylated form of the protein. Similar to endogenous KAP-1, the ectopic proteins were expressed at physiological levels, were nuclear and the wild type protein was phosphorylated on Ser 824 in response to DSBs (Fig. 2a, b). This 'protein replacement' again allowed demonstration of the strict specificity of the antibody for phosphorylated KAP-1 at early times after DSB induction (Fig. 2a, b).

Two of the cellular hallmarks of ATM deficiency are hypersensitivity to the cytotoxic effect of DSB-inducing agents and defective activation of the cell-cycle checkpoints by DSBs. Significantly, knocking down endogenous KAP-1 or its replacement by a non-phosphorylatable version of this protein (S824A) markedly increased the sensitivity of the cells to NCS (Fig. 2c). Importantly, however, the loss of the phosphorylation site of KAP-1 did not affect the activation of cell-cycle checkpoints by this treatment (see Supplementary Information, Fig. S4). The effect of DNA damage on KAP-1–KRAB transcriptional repression activity was tested using a cell line in which a *luciferase* transgene is subjected to this repression and serves as a reporter[12]. The results (data not shown) indicated that DSB induction did not affect the repressor activity assayed by this system, suggesting that KAP-1 functions in response to DNA damage in a different capacity. We also found that lack of endogenous KAP-1, or its replacement by mutant versions, did not affect phosphorylation of histone H2AX, foci formation by the damage response protein 53BP1 or ATM activation and phosphorylation of several ATM targets (see Supplementary Information, Fig. S5). Therefore, KAP-1 is not expected to function as a sensor or activator in the DNA-damage response[2] and its role in this response is downstream of ATM.

Important clues to the function of a damage-response protein can be obtained by examining its spatio-temporal dynamics following DNA damage, especially in the phosphorylated form[15]. Many ATM substrates are phosphorylated at the damage sites by chromatin-bound, activated ATM. Those participating in processes at the damage sites are retained there and form prominent nuclear foci, whereas others that function in

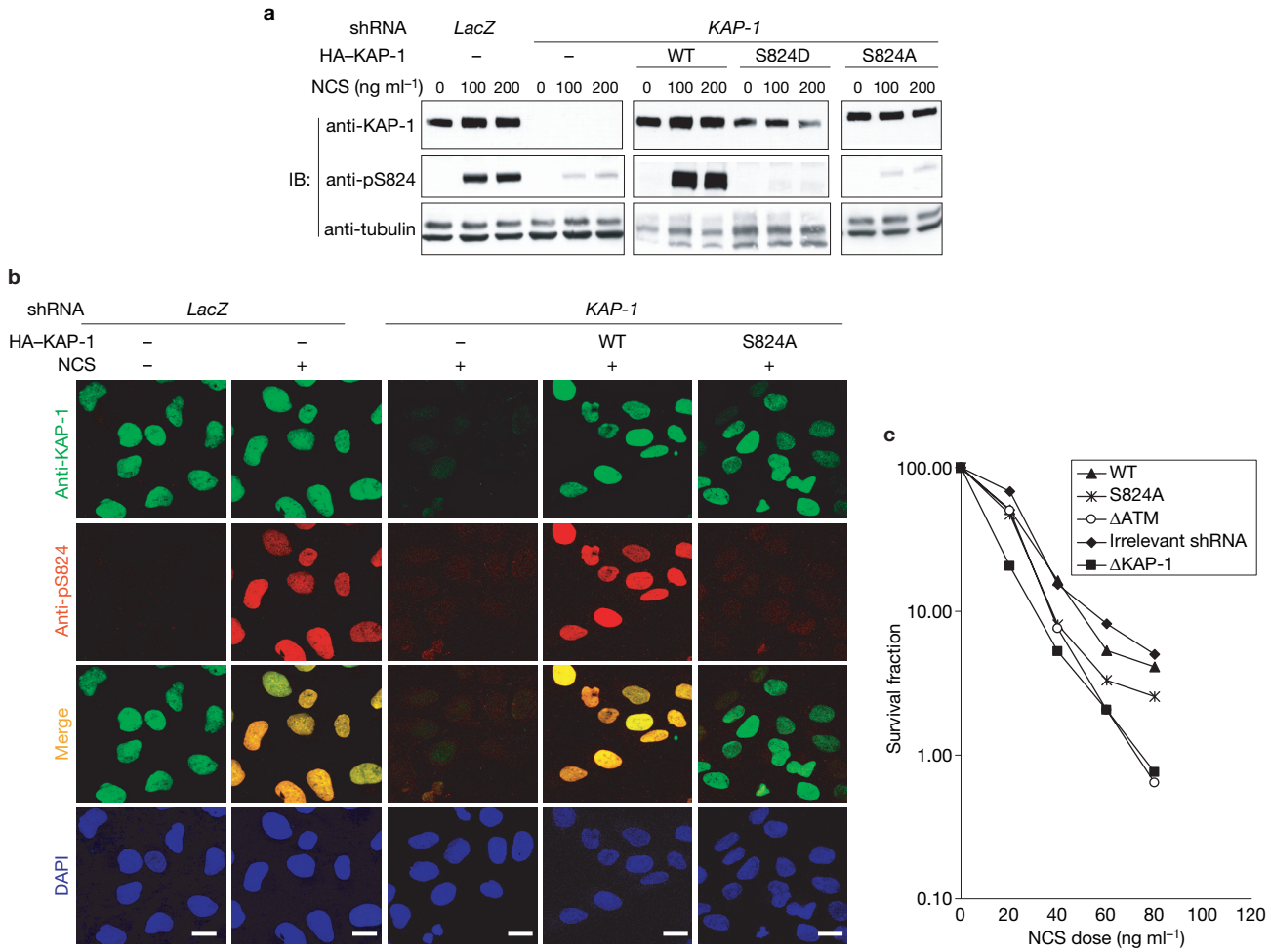

Figure 2 Functional significance of ATM-mediated phosphorylation of KAP-1 in the DNA-damage response. (**a**) Replacement of endogenous KAP-1 in U2-OS cells by ectopic protein in wild-type and two mutant versions. Protein replacement was carried out by a stable knock-down of endogenous KAP-1 and subsequent stable ectopic expression of recombinant proteins. Western blotting analysis of cellular extracts was performed after treatment of the cells with various NCS doses for 30 min. (**b**) Immunofluorescence microscopy analysis of the phosphorylation of endogenous KAP-1, and ectopic KAP-1 replacing it, in U2-OS cells. The scale bars represent 10 μm. (**c**) Loss of KAP-1 or abrogation of its phosphorylation are associated with increased sensitivity to radiomimetic treatment. U2-OS cells in which endogenous KAP-1 had been knocked down or replaced by ectopic wild-type or mutant KAP-1 proteins, and cells in which the ATM protein had been knocked down, were treated with various doses of NCS and clonogenic survival was assessed. NCS was applied to the cells using a split dose protocol (see Methods).

other locations leave these sites after their phosphorylation[15]. Spatially localized DSBs were induced in cells using micro-irradiation with a laser beam whose path across the nucleus leaves a distinct track of DSBs[15] and the spatial distribution of total and phosphorylated KAP-1 was monitored by immunofluorescence microscopy analysis. Notably, in the first few minutes after irradiation transient accumulation of KAP-1 was noticed at the damaged sites, but this rapidly disappeared (Fig. 3a). This transient stalling of KAP-1 at the damaged sites could also be observed using GFP-tagged ectopic KAP-1 (see Supplementary Information, Fig. S6). Significantly, in the first few minutes following irradiation, phosphorylated KAP-1 was confined to the DSB tracks, but then migrated quickly from the damage sites and spread throughout the nucleus, reaching pan-nuclear localization within 15 min (Fig. 3b). These results suggested that KAP-1 was transiently pausing and being phosphorylated at the DSB sites, presumably by the chromatin-bound fraction of activated ATM. Importantly, however, KAP-1 was not stably recruited to the damage sites and the phosphorylated protein rapidly diffused throughout the nucleus (Fig. 3a, b). The spatial dynamics of KAP-1 were further characterized by measuring mobility of ectopic, GFP-tagged KAP-1 using fluorescence recovery after photobleaching (FRAP) before damage induction and when its phosphorylation was maximal and pan-nuclear (see Supplementary Information, Fig. S7a). GFP–KAP-1 displayed mobility parameters typical of chromatin-associated proteins, such as HP1, in both untreated and damaged cells (see Supplementary Information, Fig. S7b, c), and this mobility was consistent with the kinetics at which the phosphorylated protein spread away from the damage sites (Fig. 3b). FRAP analysis also indicated that the phosphorylation did not alter the mobility of KAP-1 or the extent of its binding to chromatin (see Supplementary Information, Fig. S7b, c). Taken together, these results suggested that rather than functioning in processes occurring at the DSB sites, phosphorylated KAP-1 rapidly conveys a global nuclear signal, presumably associated with chromatin organization.

The notion that KAP-1 might be involved in chromatin organization also arose during cell-cycle analysis, when it was noticed that lack of KAP-1 increased the accessibility of cellular DNA to the intercalating dye propidium iodide (data not shown). This observation prompted us

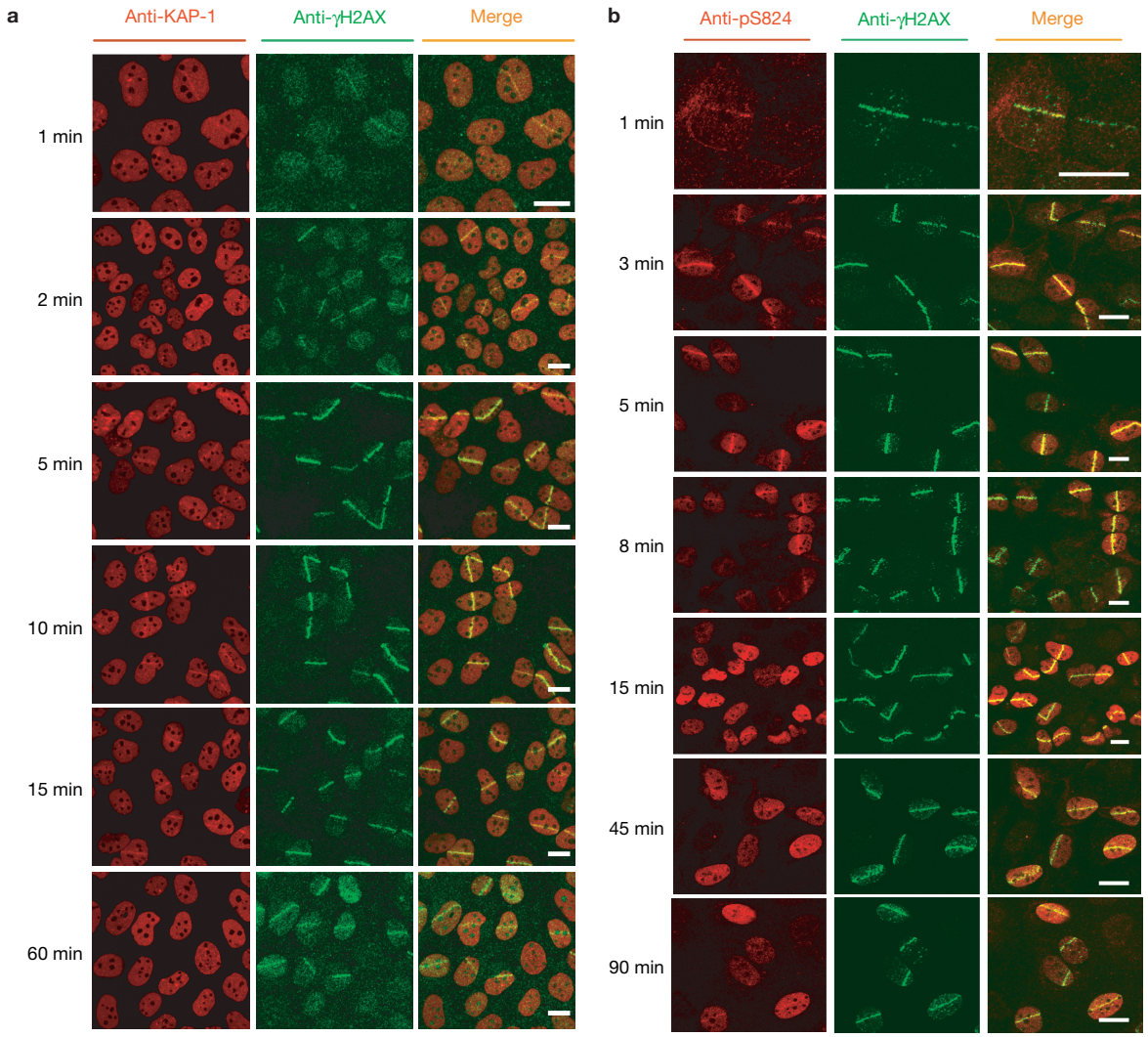

Figure 3 KAP-1 is phosphorylated at the DSB sites by chromatin bound ATM and the phosphorylated protein rapidly spreads throughout the nucleus. (**a**) Spatio-temporal dynamics of KAP-1 in response to localized DSBs. Exponentially growing U2-OS cells were exposed to a focused laser microbeam along linear tracks spanning the entire nuclear diameter. At the indicated times, the cells were fixed and immunostained with an anti-KAP-1 antibody and a monoclonal antibody against γH2AX, the phosphorylated form of histone H2AX, which marks the damage sites. Note the rapid but transient accumulation of KAP-1 at the damaged sites. (**b**) The same experiment as in Fig. 3a was performed using anti-pS824 antibodies. In the first few minutes after irradiation, KAP-1 phosphorylation is noticed exclusively at the damaged sites, but the pS824 rapidly becomes pan-nuclear. The scale bars represent 10 μm.

to examine the effect of DNA damage on the state of chromatin condensation in different KAP-1 backgrounds. Chromatin condensation was evaluated by digestion with micrococcal nuclease (MNase), which preferentially cuts the DNA in the linker regions between nucleosomes[16]. Partial MNase digestion releases chromatin fragments containing different numbers of nucleosomes; hence, the ladder obtained on gel electrophoresis of the DNA reflects the MNase accessibility of the linkers — a measure of chromatin compaction. NCS treatment caused a marked increase in cellular chromatin accessibility to MNase, which peaked in HEK293 cells approximately 1 h after treatment and largely disappeared 1 h later (Fig. 4a and see Supplementary Information, Fig. S8a), in a time course similar to that of KAP-1 phosphorylation in these cells. Significantly, this effect was noticed in cells expressing wild-type but not mutant KAP-1^{S824A} (Fig. 4b–d). Cells lacking KAP-1 exhibited a constitutive, moderate increase in MNase accessibility of their chromatin, which was reversed on expression of ectopic wild-type KAP-1 and the S824A mutant (Fig. 4e). Strikingly, when endogenous KAP-1 was replaced by the S824D mutant, the MNase accessibility of their chromatin was greater yet (Fig. 4e). These results suggested that KAP-1 is involved in maintaining chromatin condensation and pointed to a global chromatin decondensation in response to DSBs that required KAP-1 phosphorylation, presumably by inhibiting KAP-1 chromatin compaction. As KAP-1 phosphorylation is mediated by ATM, this phenomenon was examined in *ATM*-knockdown cells and was found to be ATM-dependent (Fig. 4f and see Supplementary Information, Fig. S8b). The same phenomenon was also observed in U2-OS cells (data not shown) and in the neuroblastoma cells LA-N-5 (see Supplementary Information, Fig. S8b). Interestingly, the extent of chromatin relaxation in LA-N-5 cells was greater than in HEK293 cells and its kinetics were faster. Given the magnitude of this response in LA-N-5 cells, ATM dependence was readily evident when *ATM* was knocked down in these cells (ref. 17 and see Supplementary Information, Fig. S8b). It is interesting

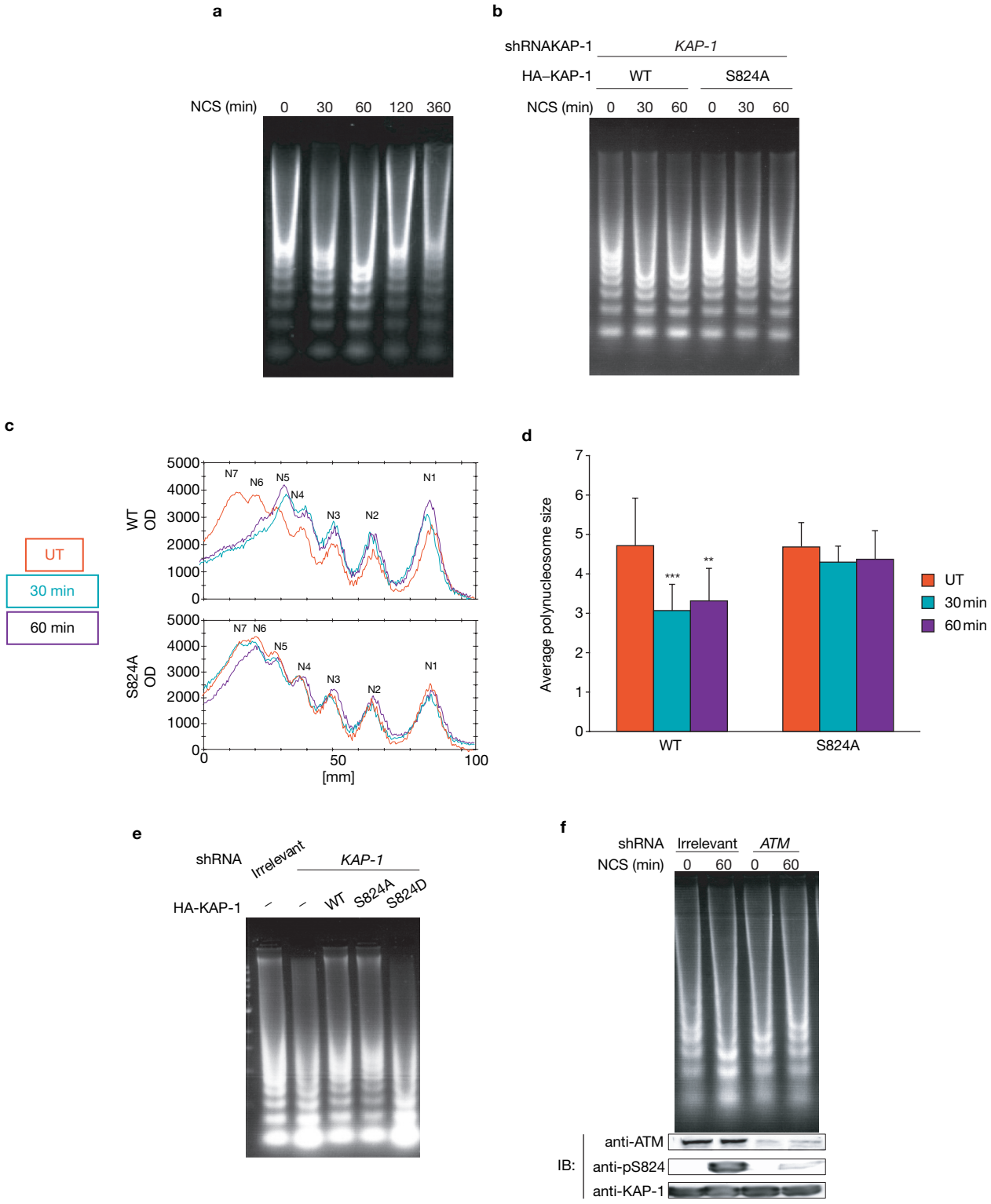

Figure 4 Chromatin relaxation in response to DSBs. (**a**) Increased MNase accessibility of chromatin at different times after treatment of HEK293 cells with 200 ng ml^{-1} of NCS. **(b)** A similar experiment as in **a** was performed with HEK293 cells in which wild-type or mutant (S824A) ectopic KAP-1 replaces the endogenous protein. The change in MNase accessibility of the chromatin is observed in cells with wild-type KAP-1 but not in those with the mutant protein. (**c**) Profiles of the various lanes of the gel presented in **b**. N1–N7 denotes the numbers of nucleosomes in each oligonucleosome. Note the shift in oligonucleosome size in wild-type cells after DNA damage. **(d)** Histogram representing average oligonucleosome length, calculated as described in the Methods, in seven independent experiments with wild-type KAP-1 and four experiments with the S824A mutant. UT: untreated control. The error bars represent the s. d. ***, $P<0.002$; **, $P<0.01$. (**e**) Comparison of basal degree of chromatin condensation in cells with different KAP-1 constitutions. Note the constitutive increase in MNase accessibility in cells lacking KAP-1 and the greater increase in chromatin relaxation associated with the S84D mutant. **(f)** ATM dependence of the DSB-induced chromatin relaxation. Comparison was made between HEK293 cells with endogenous ATM and the same cells in which *ATM* had been stably knocked down using RNAi (bottom panel).

to note that KAP-1 levels were particularly high in murine cerebellum and radiation-induced phosphorylation of KAP-1 in this tissue was particularly vigorous (data not shown).

Further evidence for DNA damage-induced chromatin decondensation was obtained using controlled digestion of chromatin with DNaseI. Although this assay is usually used for monitoring chromatin decondensation at discrete sites[18], it does demonstrate the global increase of DNA accessibility to DNaseI in the chromatin of NCS-treated cells (see Supplementary Information, Fig. S8d).

DNA damage is a major insult that induces a wide range of processes throughout the cell. At the DNA level, damage processing and repair take place at the damage sites, although gene transcription is modulated across the genome. As genomic DNA is entangled in the highly structured chromatin, it is conceivable that the chromatin must be relaxed to allow access to DNA by the relevant proteins[19,20]. Chromatin decondensation has been extensively documented at sites of gene transcription and several transcription activators have been shown to induce large-scale chromatin relaxation[21–24]. An enduring question in the DNA-damage field has been whether chromatin undergoes decondensation following DNA damage. Evidence suggests that such a process is indeed induced by DNA damage[19,20]. Two regulators of gene transcription, Gadd45 (ref. 25) and p53 (ref. 26), were found to mediate global chromatin relaxation in response to UV damage.

Several reports have suggested that a general chromatin relaxation is also induced by DSBs[27,28], but it remains unclear whether this relaxation is confined to the damage sites or whether it is global. Recently, local chromatin relaxation at the vicinity of DSBs has been demonstrated in yeast[29] and a similar, very rapid, process, which was ATM-independent, has been shown in mammalian cells[30]. Our results suggest that further to this process in mammalian cells, DSBs induce an ATM-dependent wave of chromatin relaxation that quickly traverses the entire genome, conveyed by ATM-phosphorylated KAP-1. The quantitative phosphorylation of KAP-1 (see Supplementary Information, Fig. S2) together with its rapid diffusion throughout the chromatin (Fig. 3b), allow swift and efficient induction of chromatin relaxation on a global scale.

The functional significance of this transient chromatin relaxation is highlighted by the increased sensitivity of cells with non-phosphorylatable KAP-1 to DSB-inducing agents (Fig. 2c). It has been suggested that the radiosensitivity of A-T cells reflects a subtle defect in DSB repair that leaves a minute fraction of DSBs unsealed[31]. The global, ATM- and KAP-1-dependent chromatin relaxation that follows the local, ATM-independent relaxation[30] may create a chromatin configuration that is essential for a fully efficient repair process.

However, it is not known how the message carried by KAP-1 is delivered. Following DSB induction, major changes were not detected in the interaction between endogenous KAP-1 and HP1 proteins, the association of HP1 proteins with the chromatin fraction and HP1 mobility and the interactions of KAP-1 with the histone methyltransferase SETDB1 and the Mei-2α protein (a subunit of the NuRD deacetylase complex; data not shown). The interaction of KAP-1 with Mdm2, an inhibitor and ubiquitin ligase of p53, is known not to be affected by ionizing radiation[32]. The mechanism by which KAP-1 phosphorylation leads to chromatin relaxation may depend on changes in unknown interactions of phosphorylated KAP-1 with other proteins.

Importantly, the role of KAP-1in the DNA damage response seems to be broader than its documented role as transcriptional corepressor. This is reminiscent of the transcription regulators Gadd45 and p53 (which are implicated in UV-induced chromatin relaxation[25,26]), the Brca1 and E2F1 proteins (which are also capable of regulating transcription and inducing large-scale chromatin unfolding[22]) and the transcription factor ATF2 (which when targeted by ATM functions in the DNA damage response in a transcription-unrelated capacity[33]). In this regard, it has been suggested that the transcription machinery may function in DNA damage surveillance across the genome[34]. Temporary decondensation of chromatin might facilitate such rapid genomic surveillance. This dual function may characterize additional players in the DNA damage response as this ever-expanding network continues to unfold. □

METHODS

Cell lines. HEK293 and U2-OS cells were grown in DMEM with 10% fetal bovine serum at 37 °C in 5% CO_2 atmosphere.

Antibodies. The anti-53BP1 antibody was a generous gift from T. Halazonetis (Wistar Institute, Philadelphia, PA). Other antibodies were purchased from the following manufacturers: anti-Mdm2 (OP46), Merck Biosciences, Inc. (Darmstadt, Germany); polyclonal anti-KAP-1, Bethyl Laboratories, Inc., (Montogomery, TX); monoclonal anti-KAP-1(anti-KRIP), BD Biosciences (San Jose, CA); monoclonal anti-HA, Santa Cruz Biotechnology, Inc. (Santa Cruz, CA); anti-Flag (M5) and anti-tubulin, Sigma-Aldrich (St Louis, MO); anti-pS139-H2AX, Upstate Biotechnology, Inc. (Waltham, MA). The antibody against phosphorylated Ser 407 of Mdm2 was previously described[8]. The specific phospho-antibody against phosphorylated Ser 824 of KAP-1 (BL-1067) was produced by Bethyl Laboratories, Inc. (Montgomery, TX). Secondary antibodies: anti-mouse and anti-rabbit IgG, Alexa 488/568/647 were purchased from Molecular Probes (Leiden, Netherlands), and HRP-conjugated anti-rabbit IgG or anti-mouse IgG were obtained from Jackson Immunoresearch Laboratories, Inc. (West Grove, PA).

Vectors and constructs. Full-length *KAP-1* cDNA cloned in pCMV–SPORT6 was obtained from Research Genetics (catalog #FL1001; accession number, AL552369). An HA-tag was introduced at the amino terminus of the protein expressed from this clone by inserting a synthetic oligonucleotide duplex at the *EcoR*I site of the vector. The construct expressing Flag-tagged KAP-1 in pcDNA3.0 vector was previously described[12].

***ATM* knockdown.** All stable knockdowns were obtained by expressing various shRNAs in cells using the retroviral vector pRetroSuper (a gift from R. Agami, Netherlands Cancer Institute, Amsterdam, The Netherlands). *ATM* was knocked down in HEK293 and U2-OS cells by expressing in them two shRNAs containing sequences that correspond to positions 1266–1284 of the *ATM* ORF (GATACCAGATCCTTGGAGA; obtained from R. Agami) and positions 7218–36 of this transcript (CTGGTTAGCAGAAACGTGC). The *ATM* shRNA in LA-N-5 cells contained a sequence corresponding to positions 912–932 (GACTTTGGCTGTCAACTTTCG)[17].

Stable protein replacement. An shRNA containing a sequence corresponding to positions 928–946 of *KAP-1* mRNA (GCATGAACCCCTTGTGCTG) was stably expressed in U2-OS and HEK293 cells using the pRETRO-SUPER vector. Cells were infected with retroviral particles according to standard protocols and underwent selection with 15 μg ml^{-1} (U2-OS) or 10 μg ml^{-1} (HEK293) puromycin for 6–7 days. These cells were subsequently complemented with the retroviral vector pCLXSN (RetroMax system; IMGENEX, San Diego, CA) or the retroviral vector pEGFP-C1 (BD Biosciences, Palo Alto, CA) expressing HA-tagged KAP-1, and underwent selection with 250 ng ml–^{1} neomycin. To allow the ectopic protein to be produced on the background of the stably expressed siRNA, a silent mutation, A936G), was introduced into the cDNA using the QuickChange Site-Directed Mutagenesis kit (Stratagene, La Jolla, CA).

Survival assay. U2-OS-derived cells were plated in triplicate at densities of 100–2000 cells per 60 mm plate and incubated for 48 h before exposure to various NCS doses. A 'split-dose' protocol was applied: each NCS dose was split into 15 ng ml^{-1} portions applied at 24 h intervals for up to 5 days. Cell colonies grown for

two weeks were fixed and stained with 2% crystal violet in 50% ethanol. Colonies containing at least 50 cells were counted under a dissection microscope.

Laser-induced, localized DNA double strand breaks. Cells grown on Cellocate coverslips (Eppendorf, Hamburg, Germany) were sensitized with 10 μM BrdU (Sigma, St Louis, MO) for 24 h. For micro-irradiation, the cells were placed in a LabTek chamber (Nunc, Denmark) and mounted on the stage of an Axiovert 200M microscope integrated with the Palm microlaser Workstation (P.A.L.M. Laser Technologies, Bernried, Germany). A pulsed nitrogen laser (30 Hz, 337 nm) coupled to the epifluorescence path of the microscope was focused through a LD 40×, NA 0.6 Achroplan objective to yield a spot size of approximately 1 μM. Operation was assisted by the PALMRobo-Software supplied by the manufacturer. The laser output was set to 55% to generate strictly localized and clearly tractable subnuclear DNA damage. Typically, an average of 150 cells were micro-irradiated within 10–15 min, and each cell was exposed to the laser beam for less than 500 ms. Cells were fixed at the indicated times and further processed for immunofluorescence microscopy analysis. To analyse phosphorylation of KAP-1 at very early times after irradiation, neighboring cells were laser treated along a straight line in a precisely defined region across the coverslip and fixed immediately after microirradiation of the last cell.

Immunofluorescence microscopy. U2-OS cells grown on 22-mm^2 glass coverslips to about 70% confluence were treated with 200 ng ml^{-1} NCS or microbeam irradiated (see below). Cells were fixed in 4% buffered paraformaldehyde for 10–15 min followed by a 5–10 min incubation in PBS containing 0.2–0.5% Triton X-100. Coverslips were blocked for 15 min with 1% bovine serum albumin and 10% normal donkey serum in PBS. Coverslips were incubated for 1–1.5 h with primary antibodies diluted either in primary antibody dilution buffer (Biomeda Corp., Foster City, CA; after NCS treatments) or in DMEM containing 10% fetal bovine serum (after microbeam irradiation), washed and incubated with secondary antibody for 0.5 h. All steps were carried out at room temperature and the coverslips were rinsed three times with PBS after each step.

Micrococcal nuclease digestion of chromatin. The assay was carried out as previously described[35]. Briefly, cells were harvested and nuclei immediately isolated using hypotonic buffer. Freshly isolated nuclei (1×10^7) were digested at 25 °C with MNase (Roche Applied Science, Mannheim, Germany) at a concentration of 5 U per 250 μl of digestion buffer (15 mM Tris–HCl at pH 7.4, 60 mM KCl, 15 mM NaCl, 0.25 M sucrose, 1 mM $CaCl_2$ and 0.5 mM DTT). Aliquots (50 μl) were sampled every 2 min for 10 min. Genomic DNA was purified and separated by electrophoresis in 1.2% agarose gel. Each lane of the ethidium bromide-stained gels was scanned and profiles representing band intensity were obtained using the TINA software (version 2.07D). Oligonucleosome average size was calculated as previously described[35]. Briefly, average nucleosome size is $\Sigma_{N1\text{-}Ni}(Ni\,P_{Ni})$, where Ni is the oligonucleosome size (expressed as number of nucleosomes) and P_{Ni} is the fraction of that oligonucleosome out of the total scan calculated as the ratio of the area under the oligonucleosome peak to the area of the entire scan. Statistical significance of the differences in average oligonucleosome size between the different groups was determined using the Student's *t*-test.

Note: Supplementary Information is available on the Nature Cell Biology website.

ACKNOWLEDGEMENTS

We thank M. Oren for alerting us to the DSB response detected by the anti-pS407–Mdm2 antibody, R. Agami for the pRETRO-SUPER vector and one of the sequences used to knock down ATM, Y. Lerenthal for establishing the *ATM* knockdown HEK293, S. Biton for establishing the *ATM* knockdown LA-N-5 cells, T. Halazonetis for a gift of anti-53BP1 antibodies and L. Mittelman for expert assistance with confocal microscopy. This work was supported by research grants from the A-T Children's Project, The A-T Medical Research Foundation, The National Institutes of Health (NS31763), the A-T Medical Research Trust, The A-T Ease Foundation, The European Union, the Danish National Research Foundation, and the John and Birthe Meyer Foundation. This work was carried out in partial fulfillment of the requirements for the Ph.D. degree of D.B.

COMPETING FINANCIAL INTERESTS

The authors declare that they have no competing financial interests.

Published online at http://www.nature.com/naturecellbiology/

Reprints and permissions information is available online at http://npg.nature.com/reprintsandpermissions/

1. Bassing, C. H. & Alt, F. W. The cellular response to general and programmed DNA double strand breaks. *DNA Repair* **3,** 781–796 (2004).
2. Shiloh, Y. The ATM-mediated DNA-damage response: taking shape. *Trends Biochem. Sci. doi:10.1016/j.tibs.2006.05.004* (2006).
3. Friedman, J. R. *et al.* KAP-1, a novel corepressor for the highly conserved KRAB repression domain. *Genes Dev.* **10,** 2067–2078 (1996).
4. Le Douarin, B. *et al.* A possible involvement of TIF1α and TIF1β in the epigenetic control of transcription by nuclear receptors. EMBO J **15,** 6701–6715 (1996).
5. Shiloh, Y. ATM and related protein kinases: safeguarding genome integrity. *Nature Rev. Cancer* **3,** 155–168 (2003).
6. Bakkenist, C. J. & Kastan, M. B. Initiating cellular stress responses. *Cell* **118,** 9–17 (2004).
7. Shechter, D., Costanzo, V. & Gautier, J. Regulation of DNA replication by ATR: signaling in response to DNA intermediates. *DNA Repair* **3,** 901–908 (2004).
8. Shinozaki, T., Nota, A., Taya, Y. & Okamoto, K. Functional role of Mdm2 phosphorylation by ATR in attenuation of p53 nuclear export. *Oncogene* **22,** 8870–8880 (2003).
9. Moosmann, P., Georgiev, O., Le Douarin, B., Bourquin, J. P. & Schaffner, W. Transcriptional repression by RING finger protein TIF1β that interacts with the KRAB repressor domain of KOX1. *Nucleic Acids Res.* **24,** 4859–4867 (1996).
10. Kim, S. S. *et al.* A novel member of the RING finger family, KRIP-1, associates with the KRAB-A transcriptional repressor domain of zinc finger proteins. *Proc. Natl Acad. Sci. USA* **93,** 15299–15304 (1996).
11. Reymond, A. *et al.* The tripartite motif family identifies cell compartments. *EMBO J.* **20,** 2140–2151 (2001).
12. Schultz, D. C., Ayyanathan, K., Negorev, D., Maul, G. G. & Rauscher, F. J., 3rd. SETDB1: a novel KAP-1-associated histone H3, lysine 9-specific methyltransferase that contributes to HP1-mediated silencing of euchromatic genes by KRAB zinc-finger proteins. *Genes Dev.* **16,** 919–932 (2002).
13. Ayyanathan, K. *et al.* Regulated recruitment of HP1 to a euchromatic gene induces mitotically heritable, epigenetic gene silencing: a mammalian cell culture model of gene variegation. *Genes Dev.* **17,** 1855–1869 (2003).
14. Cammas, F., Mark, M., Dolle, P., Chambon, P., Losson, R. Mice lacking the transcriptional corepressor TIF1β are defective in early post implantation development. *Development* **127,** 2955–2963 (2000).
15. Lukas, C., Falck, J., Bartkova, J., Bartek, J. & Lukas, J. Distinct spatiotemporal dynamics of mammalian checkpoint regulators induced by DNA damage. *Nature Cell Biol.* **5,** 255–260 (2003).
16. Telford, D. J. & Stewart, B. W. Micrococcal nuclease: its specificity and use for chromatin analysis. *Int. J. Biochem.* **21,** 127–137 (1989).
17. Biton, S. *et al.* Nuclear ATM mediates the cellular response to DNA double-strand breaks in human neuron-like cells. *J. Biol. Chem.* **281,** 17482–17491 (2006).
18. Lu, Q. & Richardson, B. DNaseI hypersensitivity analysis of chromatin structure. *Methods Mol. Biol.* **287,** 77–86 (2004).
19. Gontijo, A. M., Green, C. M. & Almouzni, G. Repairing DNA damage in chromatin. *Biochimie* **85,** 1133–1147 (2003).
20. Verger, A. & Crossley, M. Chromatin modifiers in transcription and DNA repair. *Cell Mol. Life Sci.* **61,** 2154–2162 (2004).
21. Muller, W. G., Walker, D., Hager, G. L. & McNally, J. G. Large-scale chromatin decondensation and recondensation regulated by transcription from a natural promoter. *J. Cell Biol.* **154,** 33–48 (2001).
22. Ye, Q. *et al.* BRCA1-induced large-scale chromatin unfolding and allele-specific effects of cancer-predisposing mutations. *J. Cell Biol.* **155,** 911–921 (2001).
23. Nye, A. C. *et al.* Alteration of large-scale chromatin structure by estrogen receptor. *Mol. Cell Biol.* **22,** 3437–3449 (2002).
24. Carpenter, A. E., Memedula, S., Plutz, M. J. & Belmont, A. S. Common effects of acidic activators on large-scale chromatin structure and transcription. *Mol. Cell Biol.* **25,** 958–968 (2005).
25. Carrier, F. *et al.* Gadd45, a p53-responsive stress protein, modifies DNA accessibility on damaged chromatin. *Mol. Cell Biol.* **19,** 1673–1685 (1999).
26. Rubbi, C. P. & Milner, J. p53 is a chromatin accessibility factor for nucleotide excision repair of DNA damage. *EMBO J.* **22,** 975–986 (2003).
27. Takahashi, K. & Kaneko, I. Changes in nuclease sensitivity of mammalian cells after irradiation with ^{60}Co γ-rays. *Int. J. Radiat. Biol. Relat. Stud. Phys. Chem. Med.* **48,** 389–395 (1985).
28. Jaberaboansari, A., Landis, M. R., Wallen, C. A. & Wheeler, K. T. Alterations of neuronal nuclear matrix and chromatin structure after irradiation under aerobic and anoxic conditions. *Radiat. Res.* **119,** 57–72 (1989).
29. Tsukuda, T., Fleming, A. B., Nickoloff, J. A. & Osley, M. A. Chromatin remodelling at a DNA double-strand break site in *Saccharomyces cerevisiae*. *Nature* **438,** 379–383 (2005).
30. Kruhlak, M. J. *et al.* Changes in chromatin structure and mobility in living cells at sites of DNA double-strand breaks. *J. Cell Biol.* **172,** 823–834 (2006).
31. Riballo, E. *et al.* A pathway of double-strand break rejoining dependent upon ATM, Artemis, and proteins locating to γ-H2AX foci. *Mol. Cell* **16,** 715–724 (2004).
32. Wang, C. *et al.* MDM2 interaction with nuclear corepressor KAP1 contributes to p53 inactivation. *EMBO J.* **24,** 3279–3290 (2005).
33. Bhoumik, A. *et al.* ATM-dependent phosphorylation of ATF2 is required for the DNA damage response. *Mol. Cell* **18,** 577–587 (2005).
34. Ljungman, M. & Lane, D. P. Transcription — guarding the genome by sensing DNA damage. *Nature Rev. Cancer* **4,** 727–737 (2004).
35. Birger, Y. *et al.* Chromosomal protein HMGN1 enhances the rate of DNA repair in chromatin. *EMBO J.* **22,** 1665–1675 (2003).
36. Ziv, Y. *et al.* Recombinant ATM protein complements the cellular A–T phenotype. *Oncogene* **15,** 159–167 (1997).

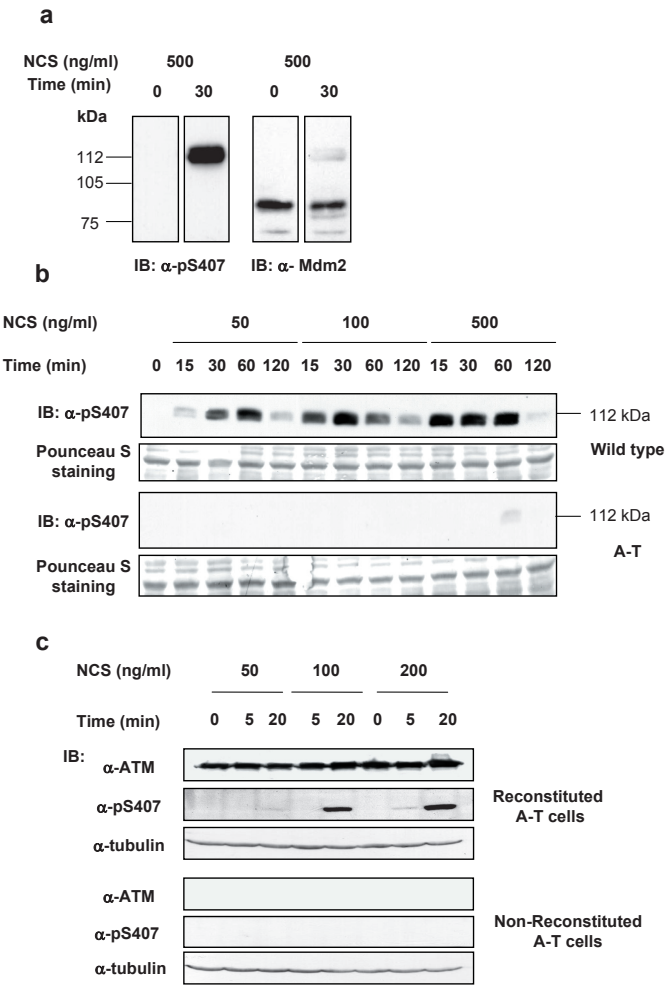

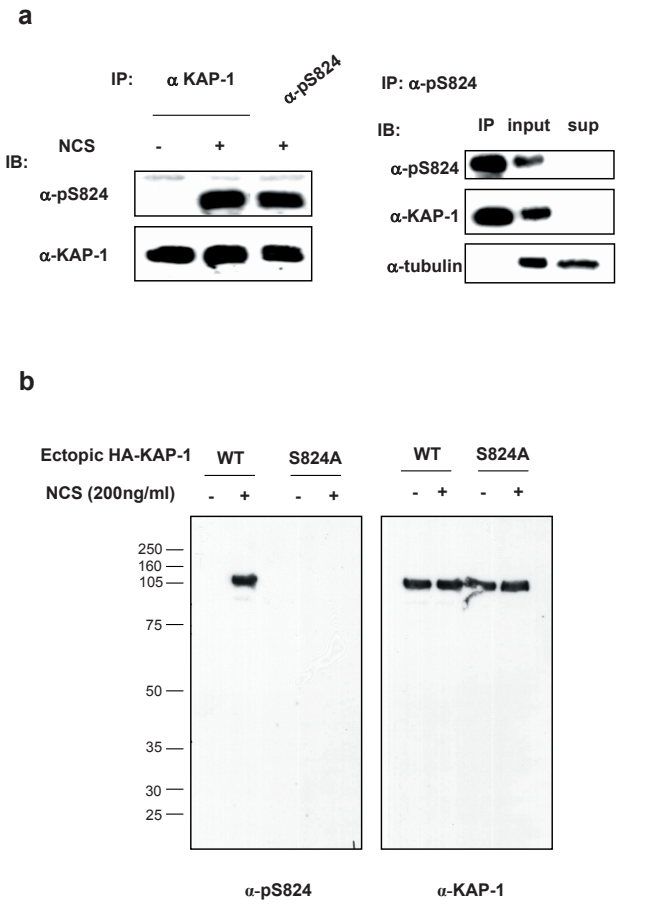

Figure S1 Characterization of the DNA damage response detected by the α-Mdm2/pS407 antibody. **a.** Western blotting analysis showing that the gel migration pattern of the protein recognized by the α-Mdm2/pS407 antibody following DSB induction is different from that of Mdm2. Lymphoblastoid cells were treated with 500 ng/ml of the radiomimetic drug NCS for 30 min and the analysis was carried out using total cellular extracts. The same blot was probed successively with the α-Mdm2/pS407 and an α-Mdm2 antibodies. **b.** Time course and ATM dependence of the reaction of the α-Mdm2/pS407 antibody with the elusive protein. Wild type and A-T lymphoblastoid cells were incubated with NCS at the indicated doses and cellular extracts were prepared at the indicated time points. **c.** Reconstitution of A-T cells with ectopically expressed ATM reconstitutes the DSB-induced signal detected by the α-Mdm2/pS407 antibody. Immortalized A-T fibroblasts (AT22IJE-T) devoid of endogenous ATM were stably reconstituted with ectopic ATM expressed from an episomal vector[36]. The cells were treated with the indicated NCS doses and processed as described above.

Figure S2 The protein whose phosphorylation is detected by the α-Mdm2/pS407 antibody is KAP-1. **a.** Reciprocal immunoprecipitations of the KAP-1 protein were carried out using an antibody against KAP-1 and the α-Mdm2/pS407 antibody. Cellular extracts of HEK293 cells treated with 200ng/ml of NCS for 30 minutes were used as source of proteins. The immune complexes were blotted consecutively with the α-Mdm2/pS407 and α-KAP-1 antibodies. Right panel: Quantitative immunoprecipitation of KAP-1 by the α-pS824 antibody using the same experimental conditions. Input: 10% of total cell extract; sup: the supernatant left after immunoprecipitation. Note the depletion of KAP-1 by the α-pS824 antibody. **b.** Western blotting analysis of total cell extracts of HEK293 cells in which endogenous KAP-1 was replaced by ectopic wild type or mutant protein. Note the specificity of the α-KAP-1 and α-pS824 antibodies.

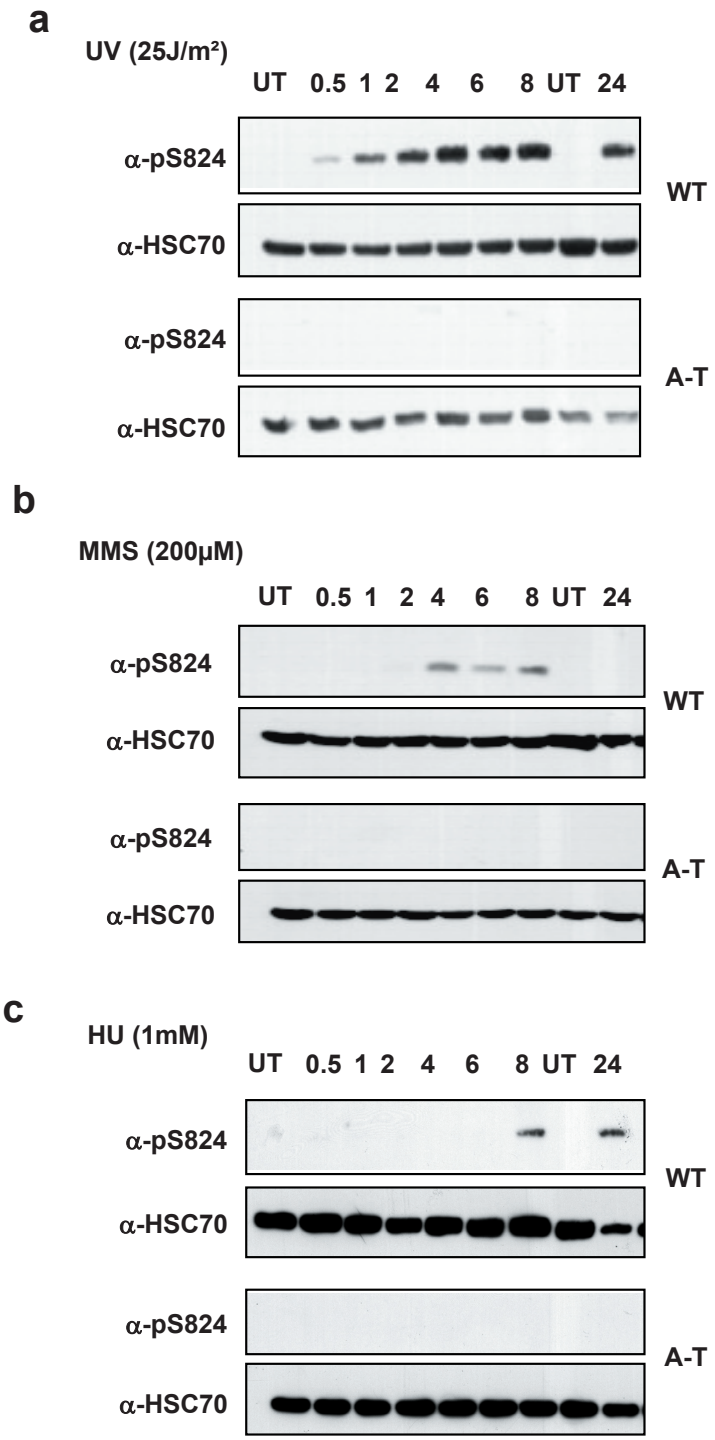

Figure S3 KAP-1 phosphorylation in response to various types of genotoxic stress. The experiment was carried out as described in Fig. 1c. The cells were treated with UV-irradiation at a dose of 25 J/M^2 (a), or with 200 μM of MMS, (b) or with 1 mM of hydroxyurea (c).

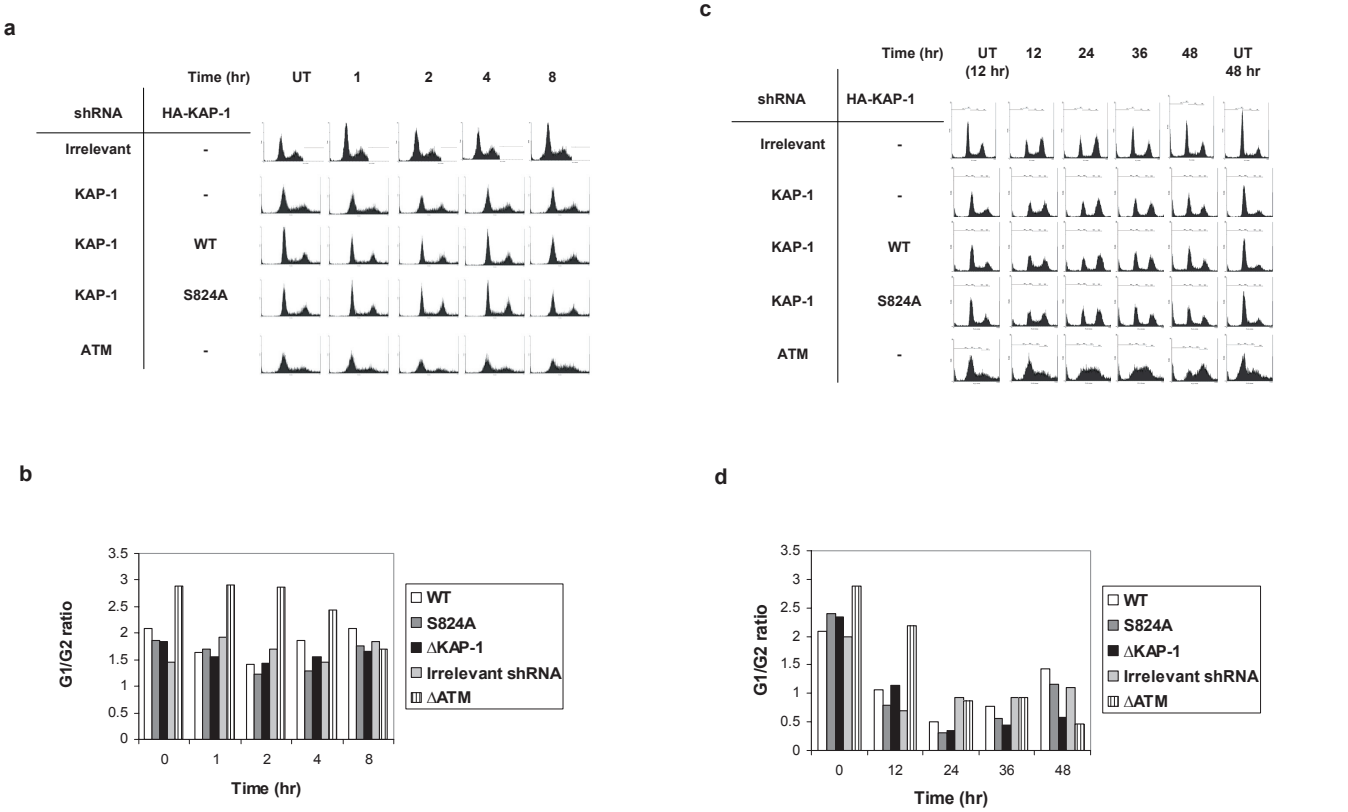

Figure S4 KAP-1 phosphorylation is not involved in DNA damage-induced activation of the cell cycle checkpoints. **a.** Flow cytometry profiles of cell cycle distribution in U2-OS cells with different KAP-1 constitutions during the first few hours after NCS treatment (100 ng/ml). DNA content (PI) is indicated at the x axis, whereas the cell count is measured at the y axis. **b.** Expression of the data shown in (a) as G1/G2 ratios. c and d. Similar analysis at extended time periods after treatment. Note the marked difference between the cell cycle distribution patterns in ATM-deficient cells and all other genotypes.

a

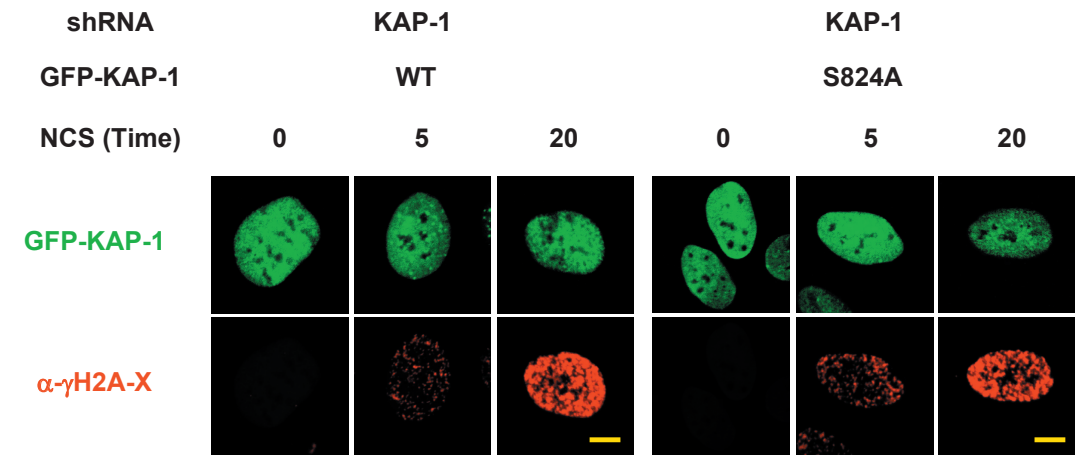

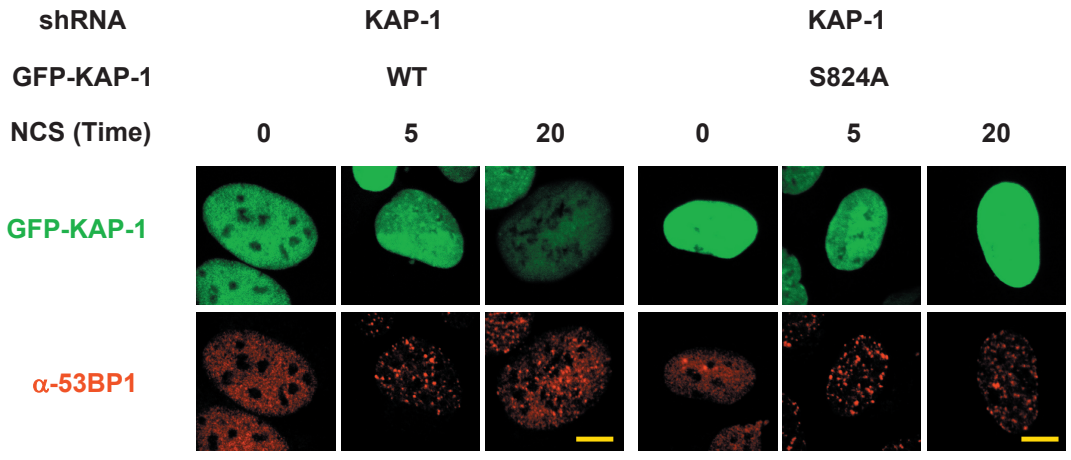

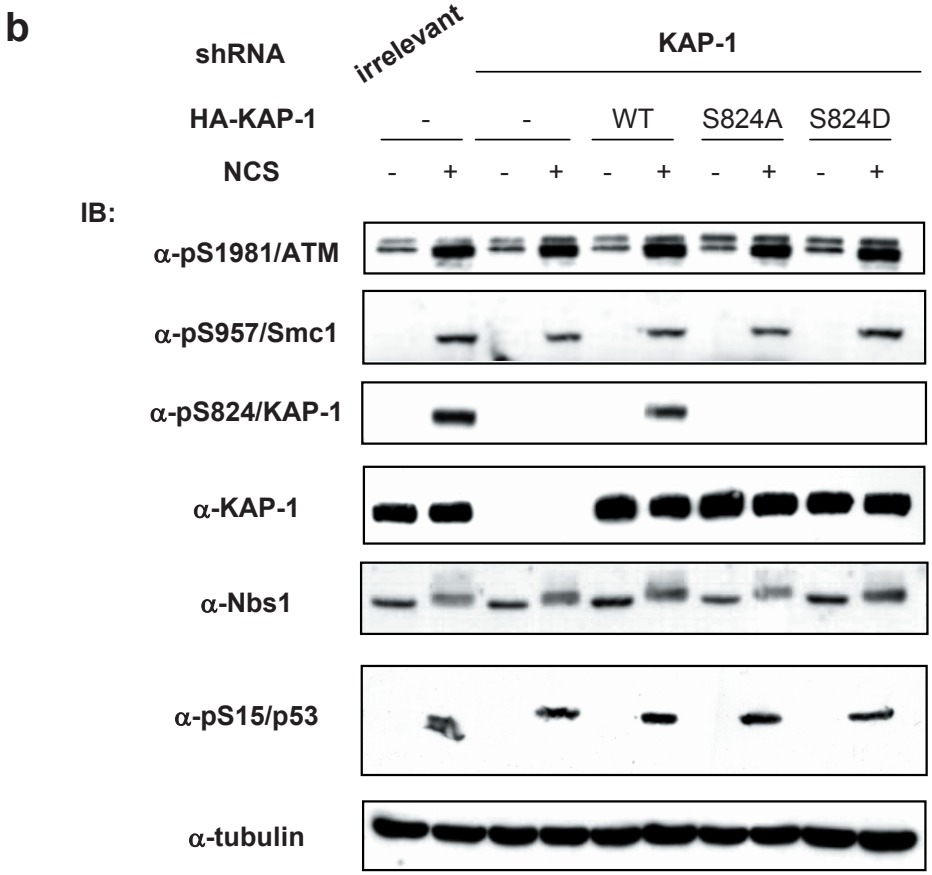

Figure S5 KAP-1 phosphorylation is not required for the early steps in the DNA damage response or the activation of ATM and downstream pathways. Experiments were carried out in U2-OS cells in which GFP-tagged, wild type or mutant (S824A) KAP-1 replaced the endogenous protein. **a.** Immunofluorescence analysis of H2AX phosphorylation (upper panel) and formation of nuclear foci by the 53BP1 protein (lower panel) after treatment with 100 ng/ml NCS for the indicated time points. Scale bars: 5μm. **b.** Western blotting analysis of cellular extracts carried out after treatment with 200ng/ml NCS for 30 min. Phosphorylation of Ser957 of the Smc1 protein and Ser15 of the p53 protein were monitored by specific anti-phospho antibodies. Nbs1 phosphorylation was monitored by following the typical band-shift of the phosphorylated protein (see ref. 2 and references therein).

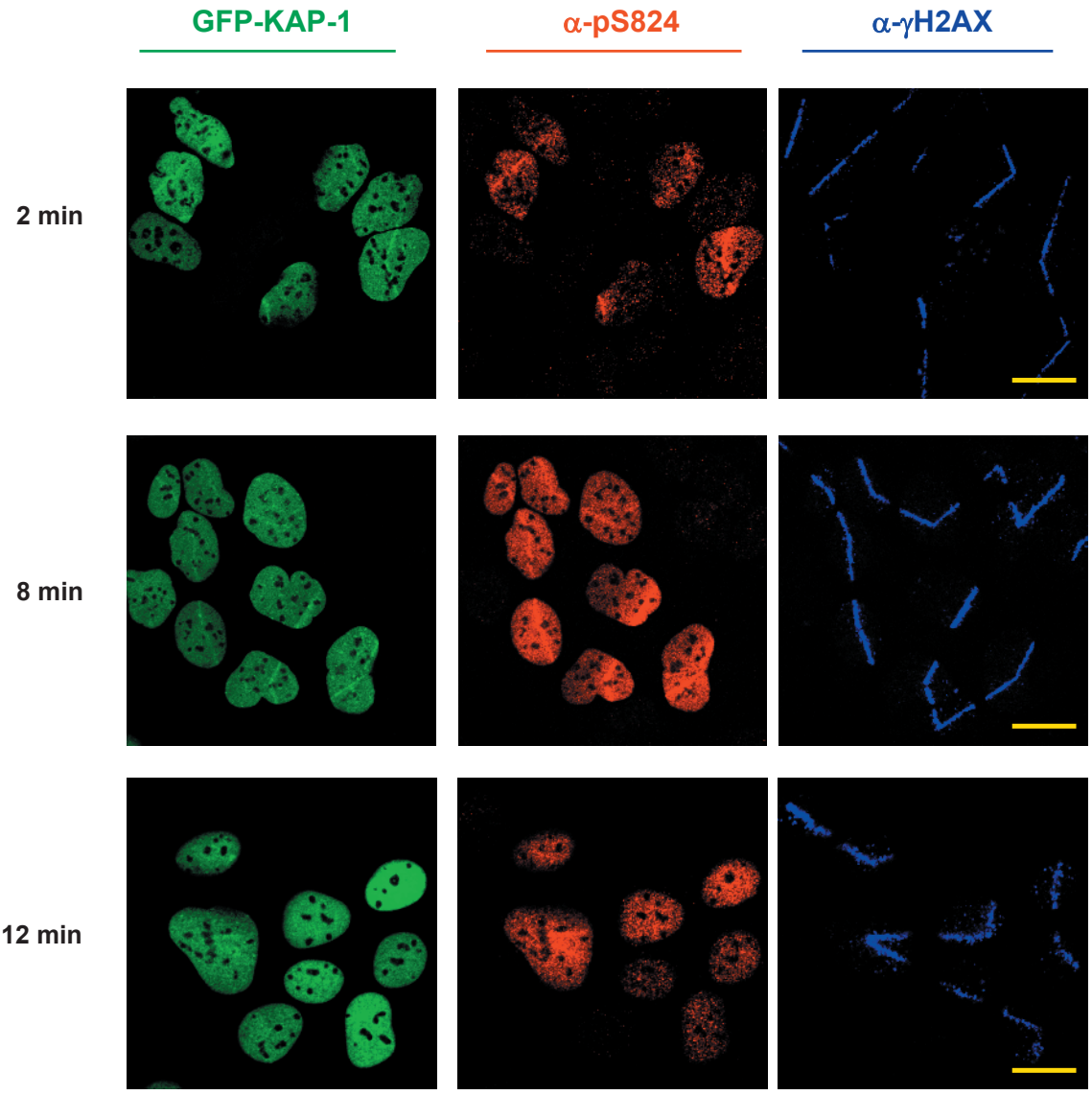

Figure S6 Temporary stalling of GFP-tagged KAP-1 at DSB sites. Spatially localized DSBs were induced as previously described in U2-OS cells expressing GFP-tagged KAP-1. In the first few minutes after damage induction a small fraction of KAP-1 accumulates at the damage sites but this phenomenon is not further observed as higher fraction of KAP-1 becomes phosphorylated. Presumably KAP-1 molecules that are already phosphorylated and traverse the damage sites do not stall for phosphorylation hence the transient accumulation of KAP-1 at these sites is detectable only at early time points after damage induction. Scale bars: 10μm.

a

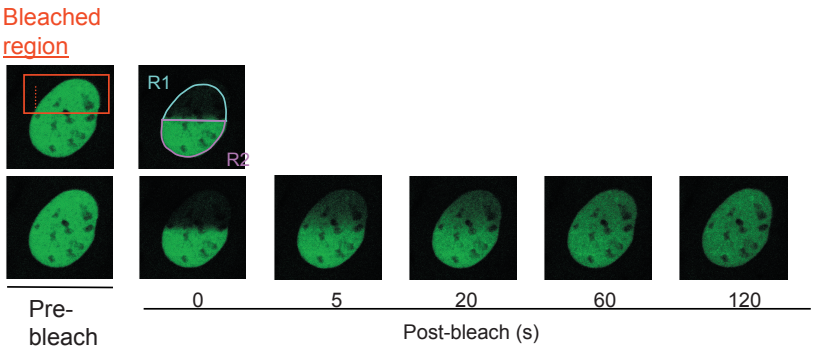

b

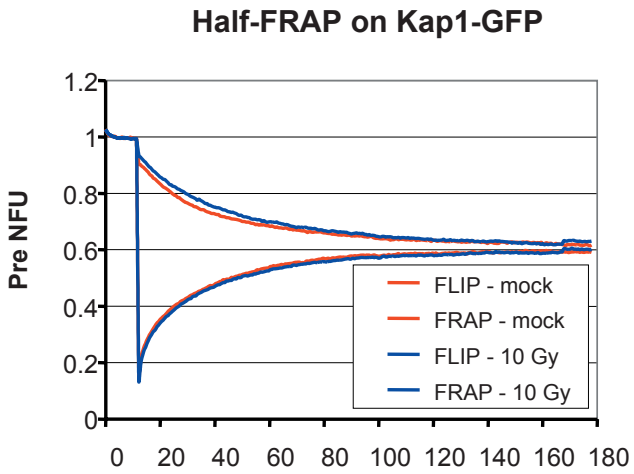

Populations	Mock		Gamma	
	Relative Abundance	Association T_{mean}	Relative Abundance	Association T_{mean}
Immobile	3.5 % ± 5.1	–	3.4 % ± 3.1	–
Unbound	5.3 % ± 4.2	–	5.5 % ± 1.6	–
Fast	26.8 % ± 0.9	2.1 s. ± 0.1	28.0 % ± 0.6	2.2 s. ± 0.1
Slow	64.1 % ± 0.8	27.1 s. ± 0.9	63.2 % ± 0.5	29.3 s. ± 0.3

Figure S7 Intra-nuclear mobility and chromatin binding properties of KAP-1. **a.** A typical example of a FRAP/FLIP assay performed in U2-OS cells in which endogenous KAP-1 was replaced by GFP-tagged KAP-1. A region (R1) spanning half of the nucleus was exposed to a single bleach pulse (see Supplementary Methods). Subsequently, the fluorescence intensities within the bleached region (R1) and in the control non-bleached region (R2) were monitored for the indicated time. The GFP signal uniformly recovers across the bleached compartment (R1), implying that the nucleus resembles a well-mixed compartment for KAP-1. b. The same cells as in (a) were exposed to 10 Gy of IR or left untreated, and subjected to the half-FRAP assay as in (a). Normalized fluorescence intensities for the bleached and unbleached areas from 10 cells were calculated and plotted along the time-scale of the experiments (180 s). The convergence of the fluorescence curves representing the bleached and control regions indicates that the fraction of immobile KAP-1 is very low (between 3-6%; see below). Notably, no significant differences were observed between the nuclear mobility of GFP-KAP-1 in irradiated and mock-treated cells. c. Chromatin-association times of distinct GFP-KAP-1 populations were calculated assuming a mathematical model that accounts for two transiently interacting pools of the protein (see Supplementary Methods). A slow-moving fraction with a mean association time of approximately 27 seconds was the most abundant one, and a smaller and faster population was observed with a mean association time of approximately 2 seconds. These values and their distributions are broadly reminiscent of those of a number of chromatin-associated proteins (see ref. 2 in the Supplementary Methods). Consistent with the fluorescence redistribution curves shown in (b), neither of these values was significantly altered after IR, indicating that KAP-1's mobility remains largely unaltered after DNA damage.

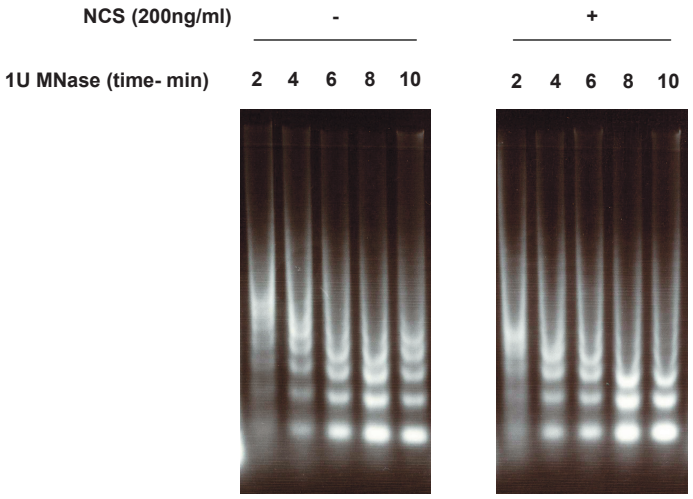

b

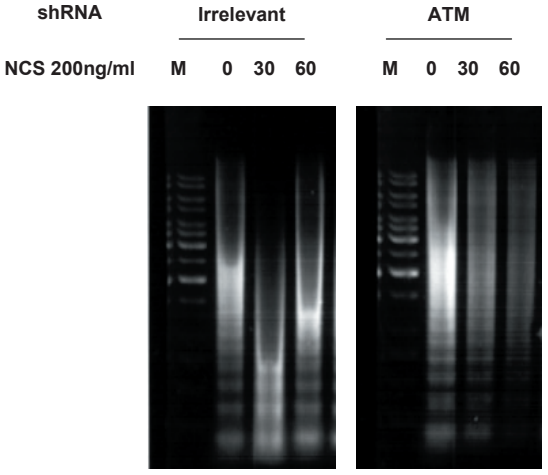

c

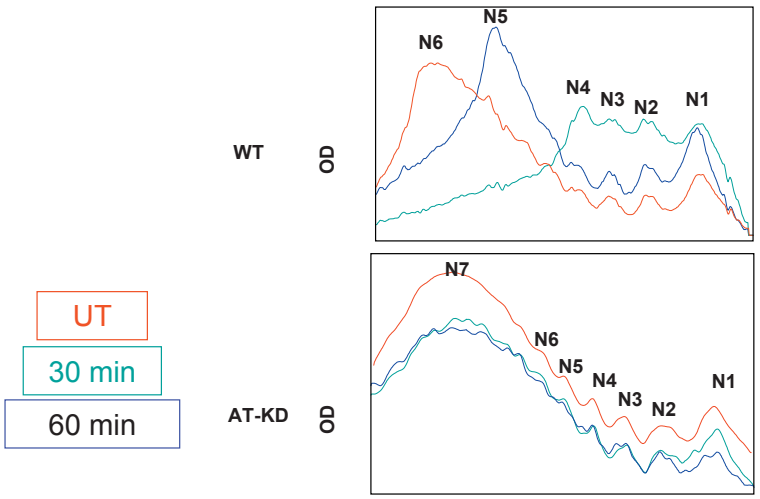

d

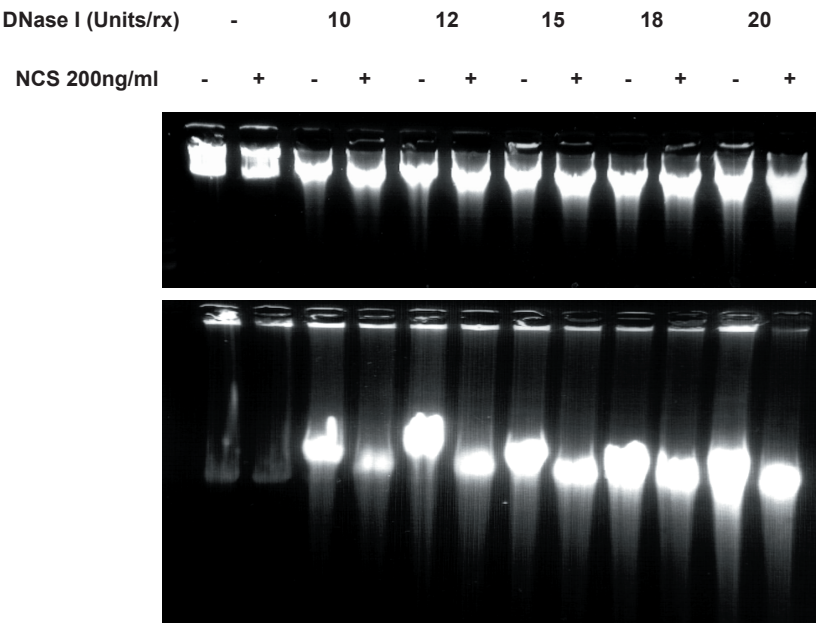

Figure S8 Chromatin relaxation in response to DSBs. **a.** Time course of partial MNase digestion of chromatin obtained from HEK293 cells, untreated (UT) or treated with 500 ng/ml of NCS for 60 min. **b.** ATM dependence of DSB-induced chromatin relaxation. ATM was knocked down using RNAi in neuroblastoma cells LA-N-5[17]. Chromatin accessibility to MNase was measured following treatment with 200 ng/ml of NCS. Note the extent and rapid kinetics of chromatin relaxation in these cells compared to HEK293 cells and the clear ATM dependence of this process. **c.** Scan profiles of the gel in Fig. S8b, UT: untreated cells. N1-N7 denotes the oligonucleosome sizes. d. Partial digestion with DNaseI of chromatin obtained from HEK293 cells, which were untreated or treated with 200 ng/ml NCS for 45 min. Equal loading of DNA was monitored by short time gel electrophoresis (top panel), and the same gel was then run for additional 48 hr (lower panel). Note increased DNAseI accessibility after DNA damage.

References for Supplementary Information

Phair, R. D, Gorski, S. A. & Misteli, T. Measurement of dynamic protein binding to chromatin in vivo, using photobleaching microscopy. *Methods Enzymol.* 375, 393-414 (2004).

Phair, R.D. *et al.* Global nature of dynamic protein-chromatin interactions in vivo: three-dimensional genome scanning and dynamic interaction networks of chromatin proteins. *Mol. Cell. Biol.* 24, 6393-6402 (2004).

Essers, J. *et al.* Nuclear dynamics of RAD52 group homologous recombination proteins in response to DNA damage. *EMBO J.* 21, 2030-2037 (2002).